JURNAL KIMIA VALENSI
p-ISSN: 2460-6065; e-ISSN: 2548-3013
Journal homepage: https://journal.uinjkt.ac.id/index.php/valensi
Research Article

Fabrication and Synthesis of Fluorescent Carbon Nanodots from Black Sticky Rice as a Sensor for the detection of Mg^{2+} ions

Zakarias Seba Ngara[1*], Anastasia Mamut[1], Redi Kristian Pingak[1], Albert Zicko Johannes[1], Reinner Ishaq Lerrick[2], Refli[3,4]

[1]*Physics Department, Faculty of Sciences and Engineering, University of Nusa Cendana, Indonesia*
[2]*Chemistry Department, Faculty of Sciences and Engineering, University of Nusa Cendana, Indonesia*
[3]*Biology Department, Faculty of Sciences and Engineering, University of Nusa Cendana, Indonesia*
[4]*Environemtal science, Post graduated, University of Nusa Cendana, Indonesia*

[*]*Email: zakariasngara@staf.undana.ac.id*

Article Info
Received: Marc 14, 2025
Revised: April 15, 2025
Accepted: Oct 7, 2025
Online: Nov 30, 2025

Citation:
Ngara, Z. S., Mamut, A., Pingak, R. K., Johannes, A. Z., Lerrick, R. I., & Refli. (2025). Fabrication and Synthesis of Fluorescent Carbon Nanodots from Black Sticky Rice as a Sensor for the detection of Mg^{2+} ions. *Jurnal Kimia Valensi*, 11(2), 162-169.

Doi: 10.15408/jkv.v11i2.45394

Abstract

Herein, fluorescent carbon nanodots (C-dots) with an average diameter of 5.51 nm were fabricated from black sticky rice by using the carbonization method. These C-dots have been synthesized with magnesium (Mg^{2+}) ions to investigate their potential application as probes for detecting Mg^{2+} ions. The as-obtained C-dots were characterized by their absorption (Abs), photoluminescence (PL), and FTIR spectra, as well as X-ray diffraction (XRD) patterns and transmission electron microscopy (TEM) images. According to their Absorption spectrum, the Absorption peak at 276 nm confirmed the presence of C-dots in the ethanol solution. Fortunately, the PL peak at 427 nm corresponded to their blue emission color. The XRD patterns and TEM image also confirmed the formation of an amorphous state and monodispersed spherical C-dots, respectively. When the as-prepared C-dots were synthesized with Mg^{2+} ions, the PL intensities of C-dots were quenched as the concentration of Mg^{2+} ions increased. A characteristic PL quenching of the C-dots through Mg^{2+} chelation demonstrated the sensing system's detection limit of 2.98 µM. This is the first report on the application of C-dots as sensors for detecting Mg^{2+} ions. These findings can pave the way for the large-scale application of these C-dots in sensing, bioimaging, drug delivery, and other fields.

Keywords: Black sticky rice, carbon nanodots, fabrication, magnesium ion, synthesis

1. INTRODUCTION

Magnesium (Mg) is one of the most important nutrient macro minerals. It is needed for the growth and metabolism process in the human body. In general, the function of the Mg element in the human body is as a cofactor for more than 300 enzymes[2]. It is needed to control blood pressure, myocardial contraction, and energy production. However, if the dose of Mg in the human body is insufficient and /or excessive, it can cause several diseases such as hypocalcemia, diarrhea, and hypomagnesemia [3]. Therefore, the dose monitoring of Mg^{2+} ions in both the human body and the environment is necessary to investigate their impact on the environment and human health. Several methods have been employed to measure the dose of metal ions, including inductively coupled plasma mass spectrometry[4], atomic fluorescence spectrometry [5], and potentiometry [6]. These methods have their own limitations, namely, the use of highly specialized instruments with complicated analytical processes, which are time-consuming and costly [1]. The method, which is low-cost, environmentally friendly, simple, and provides a quick response with high sensitivity for measuring the dose of metal ions, is a fluorescence-based method that utilizes the quenching of photoluminescence (PL) intensity from carbon nanodots (C-dots) after coordination with metal ions [1,7].

The C-dots are a new type of carbon-based nanomaterial with a size of less than 10 nm [8]. So far, fluorescent C-dots have been prepared from several types of organic material and their waste using a

specific method. For example C-dots from pomelo peel [7], soursop juice [9], mango peel [10], moringa oleifera [11], bamboo charcoal [12] , borassus flabellifer flowers[1], soursop peel[13], rice power[14], starch[15] and papaya peel[16]. These C-dots have unique properties such as strong PL in the ultraviolet-visible and near-infrared area[17], biocompatibility[10], high photostability[1], good solubility in water[17], and low toxicity[18]. According to the unique properties of C-dots, they have been applied in bioimaging[19], biomedicine[20], light-emitting diodes[15], photocatalysis[16], and sensors for metal ions such as ferric (Fe^{3+})[1,13], copper (Cu^{2+})[17,21], mercury (Hg^{2+})[22], and Beryllium (Be^{2+})[23]. Qin et al. demonstrated a green synthesis of fluorescent C-dots from flour and applied it to detect Hg^{2+} ions with a limit of detection (LOD) as low as 0.5 nM25[22]. Murugan and Sundramoorthy prepared blue fluorescent C-dots from Borassus flabellifer flowers and applied them to detect Fe^{3+} ions with the value of LOD as low as 10 nM[1] . Yingshuai et al. demonstrated green fluorescent C-dots from bamboo leaves for the detection of Cu^{2+} ions, with a LOD value as low as 115 nM[17]. In our laboratory, the fluorescent C-dots from soursop peel are used for the detection of Fe^{3+} ions with the value of LOD as low as 0.26 mM[13] and C-dots fronm dragon fruit peel for detection of zinc (Zn^{2+}) ions with the value of LOD as low as 3.2 µM[24]. To the best of our knowledge, the application of C-dots for the detection of Mg^{2+} ions has not been reported.

In this work, we fabricated C-dots from black sticky rice (*Oryza sativa Linn. Varglutinosa*, BSR) as a precursor using the carbonization method. The BSR was chosen because its major constituents are carbohydrates, which are a source for generating C-dots. It is a readily available precursor and has a low cost. The as-prepared C-dots emitted blue emission color and high photostability in an ethanol solution. When these C-dots were synthesized with Mg2+ ions, the PL intensity of C-dots quenched as the concentration of Mg2+ions increased. The quenching of this PL intensity indicated that these C-dots can be applied as sensors to detect Mg2+ ions with a LOD value as low as 2.98 µM. This result is the first to report the application of C-dots for detecting Mg2+ ions. Finally, the blue emission color, high photostability, and the PL quenching of these C-dots can open up a significant opportunity to explore C-dots as functional materials in various electronic devices, including sensors, bioimaging, medicine, and light-emitting diodes.

2. RESEARCH METHOD

Instruments and Materials

A UV lamp 365 nm to observe the fluorescent colour of C-dots, spectrophotometry of model JASCO UV-570 and SHIMADZU RF-6000 to measure absorption and PL spectra, a JASCO model FT/IR-4200 spectrophotometry to investigate the Tourier transform infrared (FTIR) spectrum, BrukerAXS X-ray diffractometers to measure X-ray diffraction (XRD) patterns, and transmission electron microscopy (TEM) to investigate the morphology of C-dots.

Black sticky Rice (BSR) was purchased from the traditional market in Kupang regency, East Nusa Tenggara Province, Indonesia. The chemical materials, including ethanol for analysis (Emsure, Germany), ferric chloride dihydrate (Emsure, Germany), magnesium chloride hexahydrate (Emsure, Germany), and phosphate-buffered saline (PBS), were purchased from Sumber Ilmiah Persada in Surabaya and Multiguna shop in Kupang. All these chemical materials were used without any further purification.

Fabrication of C-dots from black sticky rice

The fabrication of C-dots from BSR was performed according to Reference [14]. In a typical fabrication, BSR powder (20 g) was carbonized at 400 °C for 30 minutes. After cooling to room temperature, 0.5 g of this sample was added to 5 mL of ethanol, followed by a 1-hour sonication process to obtain a homogeneous, dark solution. Furthermore, ethanol (8mL) was added again for the centrifugation process at 3000 rpm for 30 minutes. Then, it was filtered to obtain the resultant supernatant, which contained fluorescent C-dots. To investigate the fluorescent color, these C-dots were illuminated with a UV lamp at 365 nm. Furthermore, these C-dots were further explored to investigate their optical properties, XRD patterns, morphology, and applied for the detection of Mg^{2+} ions.

Synthesis of C-dots with magnesium ions

Synthesis of C-dots with Mg^{2+} ions was performed at room temperature. Briefly, C-dots (1.5 mg/mL) dispersion in ethanol was added into 0.75 mL of PBS (1M, pH 7.0), followed by the addition of Mg^{2+} ions (100µL) with various concentrations (0-7µM). Furthermore, the spectra of PL and FTIR were measured using a Shimadzu RF-6000 spectrophotometer and a JASCO FT/IR-4200 spectrophotometer, respectively (**Scheme 1**).

3. RESULTS AND DISCUSSION

The schematic illustration of the preparation and synthesis of C-dots from BSR is shown in Scheme 1. The BSR was crushed and carbonized at 400 °C for 30 minutes to obtain a dark sample, indicating the formation of carbon to generate C-dots[14,23]. Under illumination with a UV lamp at 365 nm, the as-prepared C-dots emitted blue emission color in good

agreement with previous results[1,14]. Finally, these C-dots were explored for the detection of Mg^{2+} ions.

Characterization of the as-prepared C-dots

The morphology of the as-obtained C-dots was demonstrated in **Figure 1A**. Their morphologies are monodisperse in the spherical shape [18,25], which are presented with dots well separated from each other. Their corresponding size (d) distribution histogram is displayed in **Figure 1B**. Their size range is from 6.5 to 115 nm. Most of the diameter sizes of these C-dots are larger than 10 nm. The average diameter size and standard deviation are 52.31 and 21.92 nm, respectively. This result indicated that black sticky rice (BSR) is a good source for the synthesis of carbon nanomaterials. The diameter size of these C-dots is similar to the diameter size of C-dots from mango peel[10]. To further confirm the formation of C-dots, their XRD patterns and FTIR spectra were also investigated, as displayed in **Figure 2A** and **Figure 2B**, respectively. According to **Figure 2A**, the strong and broad diffraction peak located at 22.31° indicates an amorphous state of C-dots[18], which corresponds to their spherical shape. In the FTIR spectrum, the absorption bands at 3285 and 1662 cm−1 demonstrated the vibration of O-H and C=O bonds as hydroxyl and carbonyl groups, respectively. The O-H and C=O bonds are the main functional groups on the surface of C-dots, as displayed in the inset of Figure 2B. Therefore, the C-dots can bind metal ions or small molecules through the coordination between O-H and/or C=O groups with metal ions and/or small molecules [1]. Thus, the absorption bands at 2937, 1326, and 1027 cm−1 indicated the vibrations of C-H/N-H, C=C, and C-O bonds, respectively[1,13]. The analysis of the TEM image, XRD pattern, and FTIR spectrum confirmed the formation of C-dots from BSR.

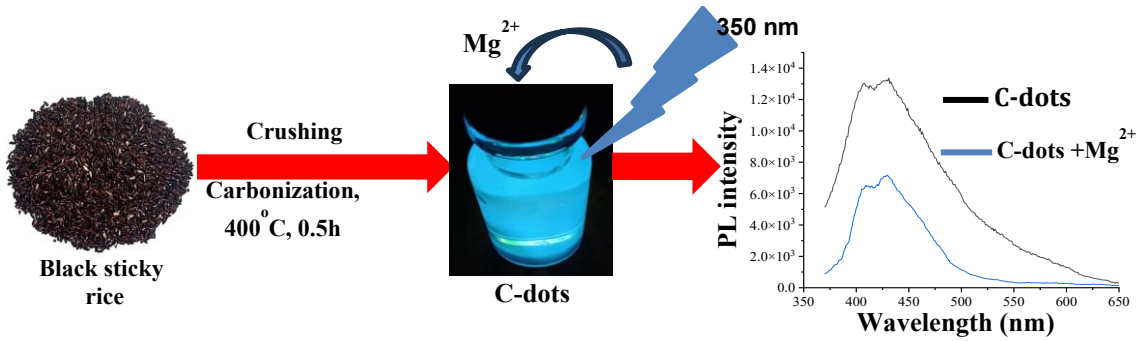

Scheme 1. The schematic illustration of preparation and synthesis of C-dots from BSR

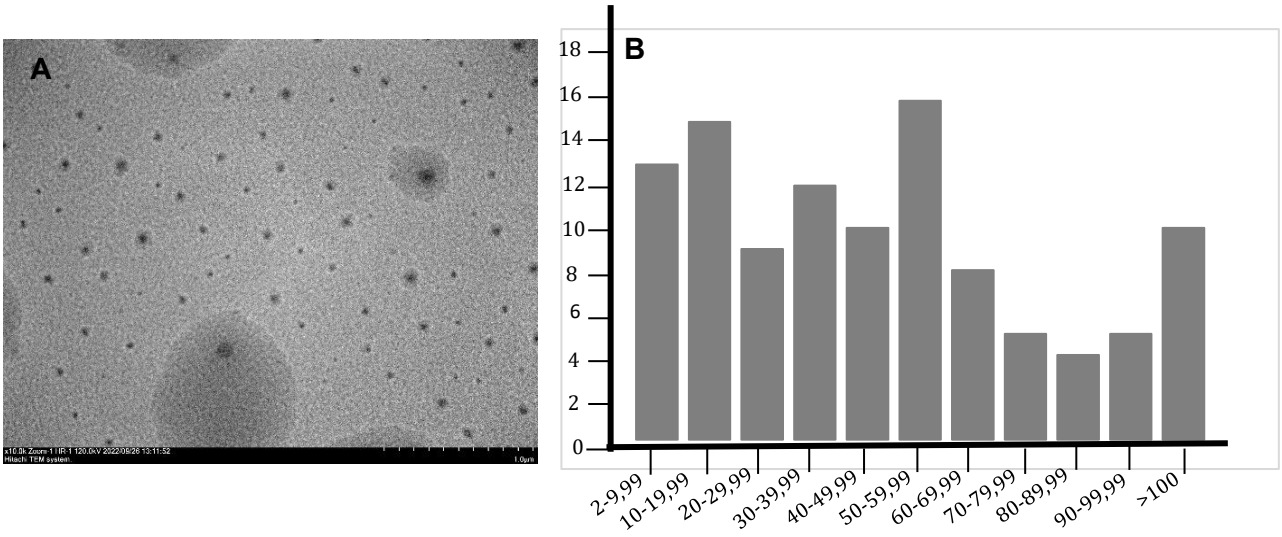

Figure 1. A) TEM image of the as-prepared C-dots, B) Size distribution of the as-prepared C-dots in histogram

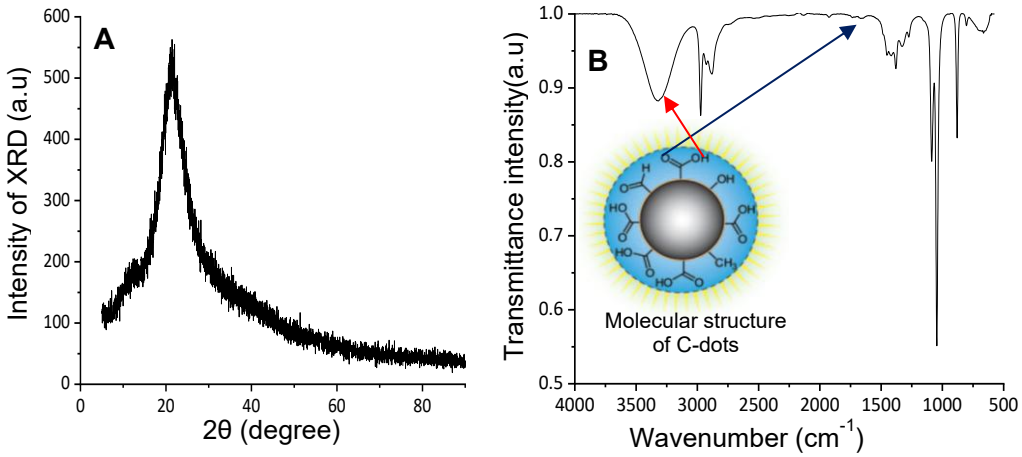

Figure 2. A) XRD patterns of C-dots, B) FTIR spectrum of C-dots. Inset show molecular structure of C-dots

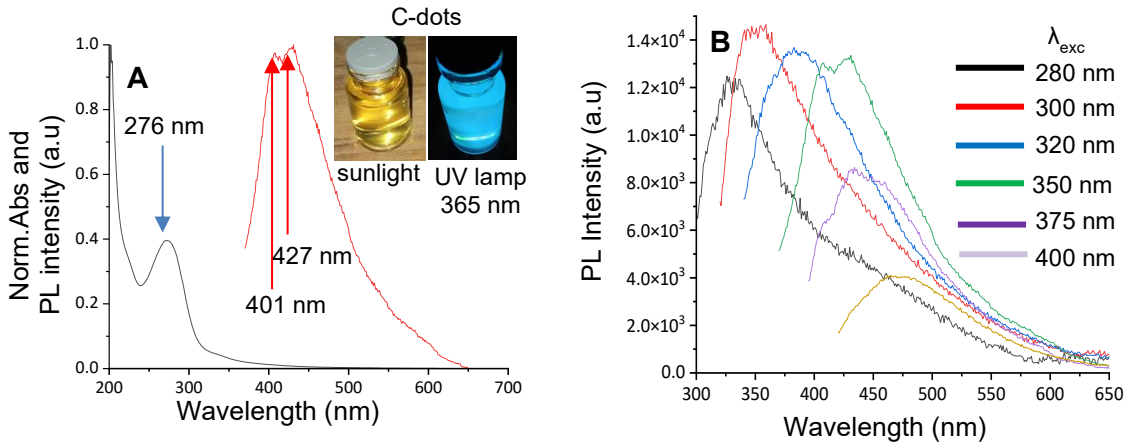

Figure 3. A) the normalization of Abs (black line) and PL (red line) spectra of the C-dots dispersion in ethanol, B) PL spectra of the C-dot depending on λ_{exc}. Inset in Figure 3A: the photographs of the C-dots dispersion in ethanol with a) sunlight and (b) UV lamp at 365 nm

Figure 3A shows the absorption (Abs) and PL spectra of the as-prepared C-dots dispersion in ethanol. According to **Figure 3A**, a clear Abs peak at 276 nm is observed, corresponding to π–π* transition of aromatic sp2 carbon from the C=C bond[26]. The inset in **Figure 3A** demonstrates photographs of the as-prepared C-dots without (a) and with (b) UV lamp at 365 nm illumination, respectively. The existence of C-dots was indicated with pale yellow by sunlight and blue fluorescence by UV lamp 365 nm illumination[8]. From the Abs spectrum, the energy gap (Eg) of the as-produced C-dots is 3.8 eV, which is smaller than that of conventional carbon (5.5 eV). The energy gap of C-dots is lower than that of conventional carbon because C-dots have a small size in nanomaterials, so the area of their absorption spectrum shifts to longer wavelengths. The shift of the absorption spectrum to longer wavelengths will produce a small energy gap in a material. Several research studies have reported results on the energy gap of C-dots. For example, the energy gap of C-dots from moringa leaves is 3.48 eV[11]. The energy gaps of C-dots from bamboo charcoal at 500 °C and 600 °C are 2.8 and 3.3 eV, respectively[12]. Upon direct excitation at an excitation wavelength (λexc) of 350 nm, the range of the PL spectrum is from 370 to 650 nm, and the PL peaks are located at 401 and 427 nm, as exhibited in Figure 3a. These PL peaks correspond with the blue fluorescence of C-dots.

To further study the optical properties of the as-obtained C-dots, we investigate the excitation-dependent PL spectra under various λexc. As shown in **Figure 3B**, the PL intensities of C-dots increase when the λexc is enhanced from 280 to 300 nm, then gradually decrease with a further increase in λexc from 300 to 400 nm. These results correspond to previous reports[18,25]. Fortunately, the PL peaks are bathochromic, ranging from 324 to 465 nm, with an enhancement of λexc from 280 to 400 nm. This is a general characteristic of C-dots[17]. The PL intensities and emission wavelength (λems) are strongly dependent on the λexc. The larger the λexc, the larger

the λems, and the lower the PL intensities. When the λexc is 350 nm, two PL peaks at 401 and 427 nm appear in the PL spectrum (**Figure 3B**, green line). In contrast, the other λexc only produces one PL peak, as displayed in Figure 3B. These results are in agreement with previous results [27,28].

Application of C-dots for detection of Mg^{2+} ions

To investigate the sensing of C-dots for the detection of metal ions, the C-dots were synthesized with metal ions. The interaction between C-dots and metal ions can occur, as indicated by the quenching of the PL intensity of C-dots with increasing metal ion concentration [1,26]. The quenching of the PL intensities meets the Stern-Volmer equation, namely F0/F = 1 + Ksv[Q][6], where Ksv is the Stern-Volmer quenching constant, which is identified as the slope of calibration graph, [Q] is the concentration of metal ions, F0 and F are PL intensities in absence and presence of different concentration of metal ions, respectively. In this research, the as-prepared C-dots were synthesized with Mg^{2+} and Fe^{3+} ions. These two metal ions were obtained from magnesium chloride hexahydrate ($MgCl_2 \cdot 6H_2O$) and ferric chloride dihydrate ($FeCl_3 \cdot 2H_2O$), respectively. According to **Figure 4A**, Mg^{2+} ions induced a strong PL quenching of C-dots, compared to Fe^{3+} ions as displayed in **Figure 4A**. The quenching of photoluminescence (PL) intensity of C-dots takes place after coordination with Mg^{2+} and Fe^{3+} ions, which is caused by energy transfer from C-dots to metal ions. Chlorine ions do not cause the PL quenching of these C-dots because the magnitude of PL quenching is not the same after C-dots coordinate with $FeCl_3 \cdot 2H_2O$ and $MgCl_2 \cdot 6H2O$. If chlorine ions cause it, the magnitude of this PL quenching is the same. Several research results on the PL quenching of C-dots caused by metal ions have been reported. They depicted that the PL quenching of C-dots occurs because energy or electron transfer takes place from C-dots to metal ions [1,7].

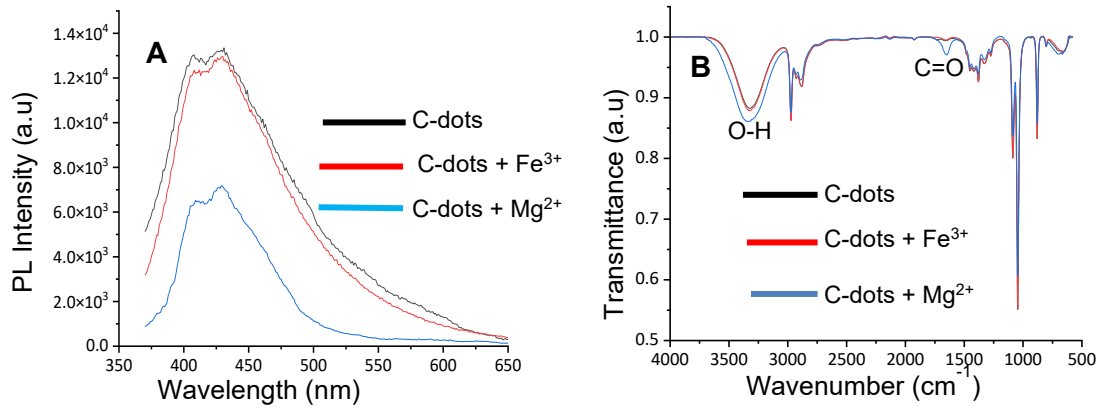

Figure 4. A) Quenching of PL intensities of the C-dots in the presence of Fe^{3+} and Mg^{2+} ions, B) FTIR spectra of C-dots (black line), C-dots + Fe^{3+} (red line), and C-dots + Mg^{2+} (blue line)

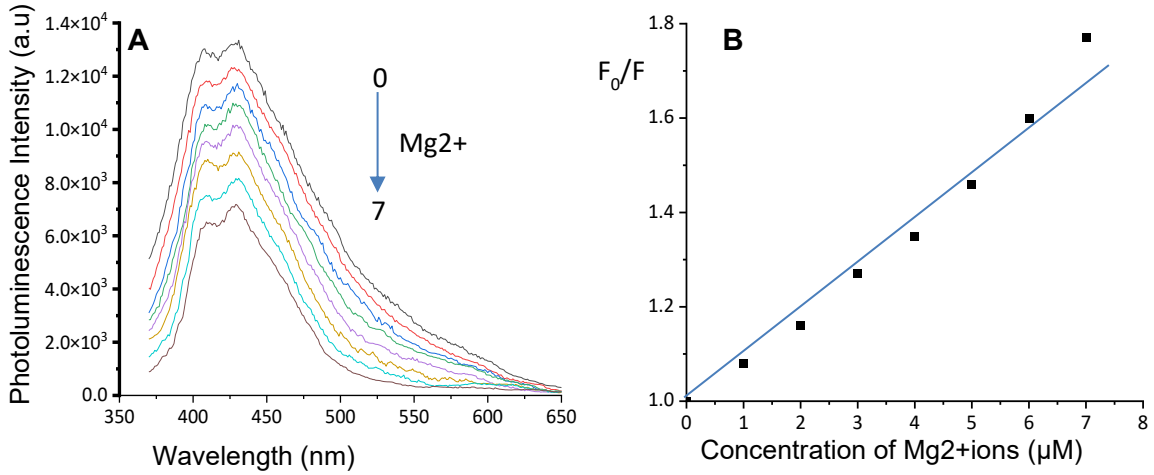

Figure 5. A) PL spectra of the C-dots in the presence of different concentration of Mg^{2+} from top to bottom: 0, 1, 2, 3, 4, 5, 6, and 7 μM, B) Plot of the F_0/F values at 427 nm versus concentration of Mg^{2+} ions (λ_{exc} at 350 nm)

In order to confirm this result, the FTIR spectrum of C-dots before and after synthesis with Mg^{2+} ions was investigated, as displayed in Figure 4B. According to **Figure 4B**, the transmittance intensity of C-dots after coordination with Mg^{2+} ions is higher and broader (blue line) than that of pure C-dots (black line). However, the transmittance intensity of C-dots after coordination with Fe^{3+} ions remains unchanged (red line). The high sensitivity of these C-dots for Mg^{2+} ions is caused by the fact that Mg^{2+} ions have a higher binding affinity and faster chelating kinetics with hydroxyl and/or carbonyl groups from C-dots6,34 than Fe^{3+} ions. In the sensing investigation, the measurement of PL spectra was performed at an excitation wavelength of 350 nm, with the PL spectrum ranging from 370 to 650 nm. The as-synthesized C-dots have the highest PL intensity around 427 nm. By increasing the concentration of Mg^{2+} ions from 0 to 7 µM, the PL intensities of C-dots at 427 nm decreased, as demonstrated in **Figure 5A**. The quenching of this PL intensity after synthesis with Mg^{2+} ions is caused by the energy or electron transfer from C-dots as donor to Mg^{2+} ions as acceptor to form a metal complex through coordination between Mg^{2+} ions and hydroxyl (O-H) or carbonyl (C=O) groups of C-dots [1,29]. Fig. 5B shows the plot of F0/F versus Q in the range from 0 to 7 µM. The linearity of the Fo/F curve to the Q indicated the excellent sensing properties of C-dots for the detection of Mg^{2+} ions. Based on **Figure 5B**, the LOD value of Mg^{2+} ions can be determined as low as 2.98 µM, which is much lower than the minimum level (6 mg/L) of Mg^{2+} ions in drinking water [30]. According to these results, these C-dots can be considered as a candidate material for the detection of Mg^{2+} ions.

4. CONCLUSION

In summary, fluorescent C-dots based on BSR have been fabricated using a carbonization method at 400 °C for 30 minutes, followed by a sonication, centrifugation, and filtration process, and then synthesized for the detection of Mg^{2+} ions. These C-dots emitted blue fluorescence and exhibited high photostability, with an indirect energy gap. The analyses of Abs, PL, and FTIR spectra, XRD patterns, and TEM Images confirmed the existence of C-dots from BSR in an ethanol solution. The synthesis of the as-produced C-dots with Mg^{2+} ions occurs, as indicated by the quenching of PL intensity from these C-dots with increasing Mg^{2+} ion concentration. The LOD value of Mg^{2+} ions was evaluated as low as 2.98 µM, which is lower than the minimum level (6 mg/L) of Mg^{2+} ions in drinking water. The quenching of the PL intensity of the as-obtained C-dots after coordination with Mg^{2+} ions demonstrated that these C-dots can be applied as a sensing for the detection of Mg^{2+} ions. These findings can pave the way for ample opportunities for application of these C-dots in sensing, bioimaging, drug delivery, and so on.

ACKNOWLEDGEMENTS

The authors greatly appreciate the financial support from Nusa Cendana University, particularly the Faculty of Science and Engineering, for this research.

REFERENCES

1. Al Alawi, A. M.; Majoni, S. W.; Falhammar, H. Magnesium and Human Health: Perspectives and Research Directions. *International Journal of Endocrinology*. Hindawi Limited 2018. https://doi.org/10.1155/2018/9041694.
2. Al Alawi, A. M.; Al Badi, A.; Al Huraizi, A.; Falhammar, H. Magnesium: The Recent Research and Developments. In *Advances in Food and Nutrition Research*; Academic Press Inc., 2021; Vol. 96, pp 193–218. https://doi.org/10.1016/bs.afnr.2021.01.001.
3. Wilschefski, S. C.; Baxter, M. R. Inductively Coupled Plasma Mass Spectrometry: Introduction to Analytical Aspects. *Clinical Biochemist Reviews* 2019, *40* (3), 115–133. https://doi.org/10.33176/AACB-19-00024.
4. Ghaedi, M.; Ahmadi, F.; Shokrollahi, A. Simultaneous Preconcentration and Determination of Copper, Nickel, Cobalt and Lead Ions Content by Flame Atomic Absorption Spectrometry. *J Hazard Mater* 2007, *142* (1–2), 272–278. https://doi.org/10.1016/j.jhazmat.2006.08.012.
5. Gupta, V. K.; Jain, A. K.; Maheshwari, G.; Lang, H.; Ishtaiwi, Z. Copper(II)-Selective Potentiometric Sensors Based on Porphyrins in PVC Matrix. *Sens Actuators B Chem* 2006, *117* (1), 99–106. https://doi.org/10.1016/j.snb.2005.11.003.
6. Murugan, N.; Sundramoorthy, A. K. Green Synthesis of Fluorescent Carbon Dots from Borassus Flabellifer Flowers for Label-Free Highly Selective and Sensitive Detection of Fe3+ Ions. *New Journal of Chemistry* 2018, *42* (16), 13297–13307. https://doi.org/10.1039/c8nj01894d.
7. Lu, W.; Qin, X.; Liu, S.; Chang, G.; Zhang, Y.; Luo, Y.; Asiri, A. M.; Al-Youbi, A. O.; Sun, X. Economical, Green Synthesis of Fluorescent Carbon Nanoparticles and Their Use as Probes for Sensitive and Selective Detection of Mercury(II) Ions. *Anal Chem* 2012, *84* (12), 5351–5357. https://doi.org/10.1021/ac3007939.

8. Abinaya, K.; Rajkishore, S. K.; Lakshmanan, A.; Anandham, R.; Dhananchezhiyan, P.; Praghadeesh, M. Synthesis and Characterization of Carbon Dots from Coconut Shell by Optimizing the Hydrothermal Carbonization Process. *Journal of Applied and Natural Science* 2021, *13* (4), 1151–1157. https://doi.org/10.31018/jans.v13i4.2916.
9. Ngara, Z. S.; Pasangka, B.; Ngana, F. R.; Elin, A. Sintesis Material Karbon Nanodots Dari Buah Sirsak Dengan Logam Besi Dan Kajian Spektrum Serapannya (Synthesis of Carbon Nanodots Material from Soursop Juice with Ferric Metal and Study on Their Absorption Spectrum). *Jurnal Fisika sains dan Aplikasinya* 2021, *6* (1), 1–7.
10. Kukreja, D.; Mathew, J.; Lakshmipathy, R.; Sarada, N. C. Synthesis of Fluorescent Carbon Dots from Mango Peels. *Int J Chemtech Res* 2015, *8* (5), 61–64.
11. Sari, E. K.; Tumbelaka, R. M.; Ardiyanti, H.; Istiqomah, N. I.; Chotimah; Suharyadi, E. Green Synthesis of Magnetically Separable and Reusable Fe3O4/Cdots Nanocomposites Photocatalyst Utilizing Moringa Oleifera Extract and Watermelon Peel for Rapid Dye Degradation. *Carbon Resources Conversion* 2023, *6* (4), 274–286. https://doi.org/10.1016/j.crcon.2023.04.003.
12. Jena, L.; Soren, D.; Deheri, P. K.; Pattojoshi, P. Preparation, Characterization and Optical Properties Evaluations of Bamboo Charcoal. *Current Research in Green and Sustainable Chemistry* 2021, *4*, 1–5. https://doi.org/10.1016/j.crgsc.2021.100077.
13. Ngara, Z. S.; Elin, A.; Ngana, F. R.; Bukit, M.; Lerrick, R. I. Facile Synthesis of Fluorescent Carbon Nanodots From Soursop Peel As a Carbon Source for Ferric Metal Ion Sensor. *Engineering and Technology Journal* 2023, *08* (10), 2904–2910. https://doi.org/10.47191/etj/v8i10.13.
14. Jaya, M.; Johanes, A. Z.; Pingak, R. K.; Ngara, Z. S. Study on Optical Properties of Carbon Nanodots by Annealing of Rice Powder as a Carbon Source. *J Phys Conf Ser* 2022, *2243* (1), 012103. https://doi.org/10.1088/1742-6596/2243/1/012103.
15. Zheng, J. X.; Liu, X. H.; Yang, Y. Z.; Liu, X. G.; Xu, B. S. Rapid and Green Synthesis of Fluorescent Carbon Dots from Starch for White Light-Emitting Diodes. *Xinxing Tan Cailiao/New Carbon Materials* 2018, *33* (3), 276–288. https://doi.org/10.1016/S1872-5805(18)60339-7.
16. Shahraki, H. S.; Bushra, R.; Shakeel, N.; Ahmad, A.; Quratulen; Ahmad, M.; Ritzoulis, C. Papaya Peel Waste Carbon Dots/Reduced Graphene Oxide Nanocomposite: From Photocatalytic Decomposition of Methylene Blue to Antimicrobial Activity. *Journal of Bioresources and Bioproducts* 2023, *8* (2), 162–175. https://doi.org/10.1016/j.jobab.2023.01.009.
17. Liu, Y.; Zhao, Y.; Zhang, Y. One-Step Green Synthesized Fluorescent Carbon Nanodots from Bamboo Leaves for Copper(II) Ion Detection. *Sens Actuators B Chem* 2014, *196*, 647–652. https://doi.org/10.1016/j.snb.2014.02.053.
18. Zhang, X.; Zhang, K.; Yao, X.; Wu, Z.; Lv, C.; Li, Q. Facile Synthesis of Blue Fluorescent Carbon Nanodots Based on the Pyrolysis of Straw for Iron (III) Detection and Cellular Imaging. *Int J Environ Anal Chem* 2020, 1–16. https://doi.org/10.1080/03067319.2020.1789612.
19. Myint, A. A.; Rhim, W. K.; Nam, J. M.; Kim, J.; Lee, Y. W. Water-Soluble, Lignin-Derived Carbon Dots with High Fluorescent Emissions and Their Applications in Bioimaging. *Journal of Industrial and Engineering Chemistry* 2018, *66*, 387–395. https://doi.org/10.1016/j.jiec.2018.06.005.
20. Sharma, A.; Das, J. Small Molecules Derived Carbon Dots: Synthesis and Applications in Sensing, Catalysis, Imaging, and Biomedicine. *J Nanobiotechnology* 2019, *17* (1), 1–24. https://doi.org/10.1186/s12951-019-0525-8.
21. Sha, Y.; Lou, J.; Bai, S.; Wu, D.; Liu, B.; Ling, Y. Hydrothermal Synthesis of Nitrogen-Containing Carbon Nanodots as the High-Efficient Sensor for Copper(II) Ions. *Mater Res Bull* 2013, *48* (4), 1728–1731. https://doi.org/10.1016/j.materresbull.2012.12.010.
22. Qin, X.; Lu, W.; Asiri, A. M.; Al-Youbi, A. O.; Sun, X. Microwave-Assisted Rapid Green Synthesis of Photoluminescent Carbon Nanodots from Flour and Their Applications for Sensitive and Selective Detection of Mercury(II) Ions. *Sens Actuators B Chem* 2013, *184*, 156–162. https://doi.org/10.1016/j.snb.2013.04.079.
23. Li, X.; Zhang, S.; Kulinich, S. A.; Liu, Y.; Zeng, H. Engineering Surface States of Carbon Dots to Achieve Controllable Luminescence for Solid-Luminescent Composites and Sensitive Be2+ Detection. *Sci Rep* 2014, *4*, 1–8. https://doi.org/10.1038/srep04976.
24. Ngara, Z. S.; Refli; Pingak, R. K.; Bukit, M.; Bernandus; Tarigan, J.; Lerrick, R. I. Characterization and Application of Fluorescent Carbon Nanodots from Dragon Fruit Peel as

Probes for Detection of Metal Ions. *Results Chem* 2025, *17*, 102522–102527. https://doi.org/10.1016/j.rechem.2025.102522.

25. Liu, Y.; Zhao, Y.; Zhang, Y. One-Step Green Synthesized Fluorescent Carbon Nanodots from Bamboo Leaves for Copper(II) Ion Detection. *Sens Actuators B Chem* 2014, *196*, 647–652. https://doi.org/10.1016/j.snb.2014.02.053.
26. Patir, K. Synthesis of Fluorescent Carbon Nanoparticles and Selective Detection of Fe 3 + in Tap Water. *IJSRST* 2018, *4* (5), 731–733.
27. Li, H.; He, X.; Liu, Y.; Huang, H.; Lian, S.; Lee, S. T.; Kang, Z. One-Step Ultrasonic Synthesis of Water-Soluble Carbon Nanoparticles with Excellent Photoluminescent Properties. *ScienceDirect* 2011, *49* (2), 605–609. https://doi.org/10.1016/j.carbon.2010.10.004.
28. Li, C. L.; Ou, C. M.; Huang, C. C.; Wu, W. C.; Chen, Y. P.; Lin, T. E.; Ho, L. C.; Wang, C. W.; Shih, C. C.; Zhou, H. C.; Lee, Y. C.; Tzeng, W. F.; Chiou, T. J.; Chu, S. T.; Cang, J.; Chang, H. T. Carbon Dots Prepared from Ginger Exhibiting Efficient Inhibition of Human Hepatocellular Carcinoma Cells. *J Mater Chem B* 2014, *2* (28), 4564–4571. https://doi.org/10.1039/c4tb00216d.
29. Basu, A.; Suryawanshi, A.; Kumawat, B.; Dandia, A.; Guin, D.; Ogale, S. B. Starch (Tapioca) to Carbon Dots: An Efficient Green Approach to an on-off-on Photoluminescence Probe for Fluoride Ion Sensing. *Analyst* 2015, *140* (6), 1837–1841. https://doi.org/10.1039/c4an02340d.
30. Rosanoff, A. The High Heart Health Value of Drinking-Water Magnesium. *Med Hypotheses* 2013, *81* (6), 1063–1065. https://doi.org/10.1016/j.mehy.2013.10.003.